

Heat transfer on a hot surface impinged by a cold circular liquid jet

Shu, Jian Jun

2010

Shu, J. J. (2010). Heat transfer on a hot surface impinged by a cold circular liquid jet. V European Conference on Computational Fluid Dynamics (5th:2010:Lisbon).

<https://hdl.handle.net/10356/94029>

© 2010 ECCOMAS CFD. This is the author created version of a work that has been peer reviewed and accepted for publication by V European Conference on Computational Fluid Dynamics. It incorporates referee's comments but changes resulting from the publishing process, such as copyediting, structural formatting, may not be reflected in this document. The official URL of the Conference is: [<http://www.eccomas-cfd2010.org/index.php>].

Downloaded on 27 Nov 2022 23:51:42 SGT

HEAT TRANSFER ON A HOT SURFACE IMPINGED BY A COLD CIRCULAR LIQUID JET

Jian-Jun SHU

School of Mechanical & Aerospace Engineering, Nanyang Technological University
50 Nanyang Avenue, Singapore 639798
e-mail: mjjshu@ntu.edu.sg

Key words: Thin film flow, Large Reynolds numbers, Modified Keller box method

Abstract. *The paper considers heat transfer characteristics of thin film flow over a hot horizontal flat plate resulting from a cold vertical jet of liquid falling onto the surface. A numerical solution of high accuracy is obtained for large Reynolds numbers using the modified Keller box method.*

1 INTRODUCTION

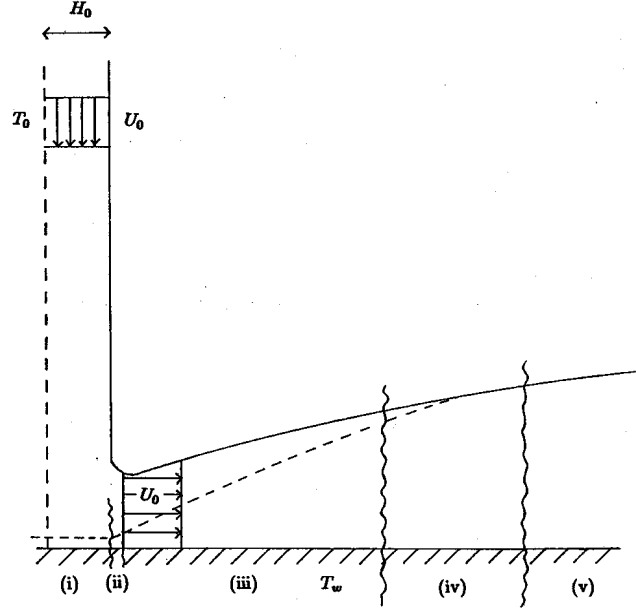
As has been noted earlier the draining flow of liquid under gravity through banks of horizontal tubes occurs frequently in technological processes involving heat or mass transfer. The mode of drainage may be in the form of droplets, columns or continuous sheets. After having examined the sheet mode of drainage, it is natural to move on to a closer inspection of the columnar mode of drainage. Again, if the film thickness is small relative to a typical tube dimension, the impact surface may be regarded as locally plane. Accordingly an initial prototype model for columnar impingement is simply that of a vertical round jet striking a plane horizontal surface. The flow model is thus axisymmetric and considerable simplification of the governing equations can be made. Some detailed understanding of the flow and heat transfer characteristics at the point of impingement may be obtained and possible methodologies identified for examining the non-axisymmetric flow in due course.

Analytically Watson [1] found a similarity solution of the boundary-layer equations governing such a flow and also considered by approximate methods the initial growth of the boundary layer from the stagnation point where the similarity solution does not hold. Chaudhury [2] obtained a supplementary thermal solution using an orthogonal polynomial. Some recent progress [3-6] has been made in investigating various problems of a liquid jet impinging on a solid surface. In this paper, an accurate numerical solution is obtained for the heat transfer in the flow of a cold, axisymmetric vertical liquid jet against a hot horizontal plate.

2 GOVERNING EQUATIONS

The problem to be examined concerns the film cooling which occurs when a cold vertically draining column strikes a hot horizontal plate. Although a column of fluid draining under gravity is accelerated and thin at impact, it is reasonable to model the associated volume flow as a jet of uniform velocity U_0 , uniform temperature T_0 and radius H_0 as is illustrated in Figure 1. The notation $Q = \pi H_0^2 U_0$ is introduced for the flow rate and a film Reynolds number may be defined as $R_e = \frac{U_0 H_0}{\nu}$ where ν is the kinematic viscosity of the fluid. When an impinging circular jet strikes a plane surface, it experiences an eventually inviscid radially symmetric division and deflection through 90° . In the immediate vicinity of the point of impact, viscous effects begin to influence the flow field. The underlying hydrodynamics of the fluid flow have been delineated [1]. Exactly the same physical assessment of the flow field applies as was outlined [3].

Figure 1: The vertical jet and resultant film for the axisymmetric flat plate



- (i) Imbedded stagnation boundary layer
- (ii) Outer inviscid deflection region
- (iii) Quasi Blasius viscous diffusion
- (iv) Transition around viscous penetration
- (v) Similarity film flow

The dashed line represents the hydrodynamic boundary layer.

The flow under investigation has been modelled as a steady, axisymmetric flow of incompressible fluid. In the absence of body forces and viscous dissipation, the equations expressing conservation of mass, momentum and energy are consequently

$$\nabla \cdot \vec{V} = 0 \quad (1)$$

$$\rho(\vec{V} \cdot \nabla)\vec{V} = -\nabla P + \mu \nabla^2 \vec{V} \quad (2)$$

$$\rho C_p (\vec{V} \cdot \nabla) T = k \nabla^2 T \quad (3)$$

where $\vec{V} = (v_r, v_z)$ are velocity components associated with cylindrical coordinates (r, z) measured along the plate from the axis of deflection and normal to the plate respectively. ρ , μ , C_p and k are the density, dynamic viscosity, specific heat at constant pressure and the thermal conductivity of the cooling fluid in the jet respectively. T and P are respectively the temperature and pressure within the fluid.

The specific boundary conditions under which the equations are to be solved closely parallel those of Shu and Wilks [3]. In particular, at the wall, the no slip condition and the constant temperature T_w require

$$v_r = v_z = 0, \quad T = T_w \quad \text{on } z = 0, \quad r \geq 0. \quad (4)$$

On the free surface, assuming negligible shear stress and heat flux, requires

$$\frac{\partial v_r}{\partial z} + \frac{\partial v_z}{\partial r} = 0, \quad \frac{\partial T}{\partial z} = 0 \quad \text{at } z = H(r), \quad r \geq 0. \quad (5)$$

The conservation of volume constraint applies at any given r station and hence

$$2\pi \int_0^{H(r)} rv_r(r, z) dz = \text{const.} = \pi H_0^2 U_0 \text{ for } r \geq 0. \quad (6)$$

Under the assumption that the film thickness remains thin relative to a characteristic horizontal dimension, a boundary layer treatment of the equations leads to significant simplification.

The following non-dimensional variables are introduced

$$x = \frac{r}{R_e^{1/3} H_0}, \quad \bar{Y} = \frac{R_e^{1/3} z}{H_0}, \quad (7)$$

$$\bar{H}(x) = \frac{R_e^{1/3} H(r)}{H_0}, \quad (8)$$

$$\bar{U} = \frac{v_r}{U_0}, \quad \bar{V} = \frac{R_e^{2/3} v_z}{U_0}, \quad \bar{\phi} = \frac{T - T_w}{T_0 - T_w}, \quad p = \frac{P}{\rho U_0^2}. \quad (9)$$

In the limit $R_e \rightarrow +\infty$ with x remaining $O(1)$, the following equations are obtained

$$\frac{\partial}{\partial x}(x\bar{U}) + \frac{\partial}{\partial \bar{Y}}(x\bar{V}) = 0 \quad (10)$$

$$\bar{U} \frac{\partial \bar{U}}{\partial x} + \bar{V} \frac{\partial \bar{U}}{\partial \bar{Y}} = -\frac{\partial p}{\partial x} + \frac{\partial^2 \bar{U}}{\partial \bar{Y}^2} \quad (11)$$

$$0 = \frac{\partial p}{\partial \bar{Y}} \quad (12)$$

$$P_r \left(\bar{U} \frac{\partial \bar{\phi}}{\partial x} + \bar{V} \frac{\partial \bar{\phi}}{\partial \bar{Y}} \right) = \frac{\partial^2 \bar{\phi}}{\partial \bar{Y}^2} \quad (13)$$

where $P_r = \frac{\nu}{\kappa}$ is the Prandtl number with ν the kinematic viscosity $\frac{\mu}{\rho}$ and κ the

thermometric conductivity $\frac{k}{\rho C_p}$. In common with standard boundary layer theory (12)

implies that the pressure across the film remains constant. In the absence of external pressure gradients and with zero shear assumed on the free surface, the pressure term in (11) is identically zero.

In non-dimensional variables the boundary conditions now read

$$\bar{U} = \bar{V} = \bar{\phi} = 0 \quad \text{on } \bar{Y} = 0, \quad x \geq 0 \quad (14)$$

$$\frac{\partial \bar{U}}{\partial \bar{Y}} = \frac{\partial \bar{\phi}}{\partial \bar{Y}} = 0 \quad \text{at } \bar{Y} = \bar{H}(x), \quad x \geq 0 \quad (15)$$

$$\int_0^{\bar{H}(x)} x \bar{U} d\bar{Y} = \frac{1}{2} \quad \text{for } x \geq 0. \quad (16)$$

3 NUMERICAL SOLUTIONS

The continuity equation (10) is eliminated by introducing a stream function ψ defined by

$$\bar{U} = \frac{1}{x} \frac{\partial \psi}{\partial \bar{Y}}, \quad \bar{V} = -\frac{1}{x} \frac{\partial \psi}{\partial x}. \quad (17)$$

Owing to the geometry, $\bar{H}(x)$ is singular at $x=0$. To remove this singularity, y and $\bar{h}(x)$ are introduced and given by

$$y = x\bar{Y}, \quad \bar{h}(x) = x\bar{H}(x). \quad (18)$$

Substituting equations (17) and (18) into (10)-(16) gives

$$\frac{\partial^3 \psi}{\partial y^3} = \left(\frac{I}{x^2} \right) \left(\frac{\partial \psi}{\partial y} \frac{\partial^2 \psi}{\partial x \partial y} - \frac{\partial \psi}{\partial x} \frac{\partial^2 \psi}{\partial y^2} \right) \quad (19)$$

$$\frac{\partial^2 \bar{\phi}}{\partial y^2} = \left(\frac{P_r}{x^2} \right) \left(\frac{\partial \psi}{\partial y} \frac{\partial \bar{\phi}}{\partial x} - \frac{\partial \psi}{\partial x} \frac{\partial \bar{\phi}}{\partial y} \right) \quad (20)$$

subject to boundary conditions

$$\psi = 0, \quad \frac{\partial \psi}{\partial y} = 0, \quad \bar{\phi} = 0 \quad \text{on } y = 0, \quad x \geq 0 \quad (21)$$

$$\psi = \frac{1}{2}, \quad \frac{\partial^2 \psi}{\partial y^2} = 0, \quad \frac{\partial \bar{\phi}}{\partial y} = 0 \quad \text{at } y = \bar{h}(x), \quad x \geq 0 \quad (22)$$

$$\bar{h} = \frac{1}{2}, \quad \psi = y, \quad \bar{\phi} = 1 \quad \text{on } x = 0, \quad 0 < y \leq \frac{1}{2} \quad (23)$$

where the initial condition (23) appears due to the original initial condition

$$H = \frac{H_0^2}{2r}, \quad v_r = U_0, \quad T = T_0 \quad \text{on } r = 0, \quad 0 < z \leq \frac{H_0^2}{2r}. \quad (24)$$

In anticipation of the use of a Keller box method and its attractive extrapolation features the differential system (19)-(23) is re-cast as the following first order system

$$\begin{aligned} \frac{\partial \psi}{\partial y} &= \bar{u} \\ \frac{\partial \bar{u}}{\partial y} &= \bar{v} \\ \frac{\partial \bar{v}}{\partial y} &= \left(\frac{I}{x^2} \right) \left(\bar{u} \frac{\partial \bar{u}}{\partial x} - \bar{v} \frac{\partial \psi}{\partial x} \right) \\ \frac{\partial \bar{\phi}}{\partial y} &= \bar{w} \\ \frac{\partial \bar{w}}{\partial y} &= \left(\frac{P_r}{x^2} \right) \left(\bar{u} \frac{\partial \bar{\phi}}{\partial x} - \bar{w} \frac{\partial \psi}{\partial x} \right) \end{aligned} \quad (25)$$

whose boundary conditions are

$$\begin{aligned}
 \psi &= 0, \bar{u} = 0, \bar{\phi} = 0 \quad \text{on } y = 0, x \geq 0 \\
 \psi &= \frac{1}{2}, \bar{v} = 0, \bar{w} = 0 \quad \text{on } y = \bar{h}(x), x \geq 0 \\
 \bar{h} &= \frac{1}{2}, \psi = y, \bar{\phi} = 1 \quad \text{on } x = 0, 0 < y \leq \frac{1}{2}.
 \end{aligned} \tag{26}$$

The following coordinate transformation, what simultaneously maps the film thickness onto the unit interval and removes the Blasius singularity at the origin, is introduced

$$x = \xi^{\frac{2}{3}}, \quad y = \frac{\xi \eta \bar{h}}{\xi + 1 - \eta}.$$

The dependent variables are transformed as

$$\begin{aligned}
 \psi &= \frac{\xi}{\xi + 1 - \eta} f, \quad \bar{u} = \frac{u}{(1 + \xi)^2}, \quad \bar{v} = \frac{\xi + 1 - \eta}{\xi(1 + \xi)^4} v, \\
 \bar{\phi} &= \phi, \quad \bar{w} = \frac{\xi + 1 - \eta}{\xi(1 + \xi)^2} w, \quad \bar{h} = (1 + \xi)^2 h
 \end{aligned}$$

The equations to be solved now read

$$\begin{aligned}
 f_\eta &= \frac{(1 + \xi)hu}{\xi + 1 - \eta} - \frac{f}{\xi + 1 - \eta} \\
 u_\eta &= \frac{(1 + \xi)hv}{\xi + 1 - \eta} \\
 v_\eta &= \frac{v}{\xi + 1 - \eta} - \frac{3\xi(1 + \xi)^2 hu^2}{(\xi + 1 - \eta)^3} - \frac{3(1 - \eta)(1 + \xi)^3 hfv}{2(\xi + 1 - \eta)^4} \\
 &+ \frac{3\xi(1 + \xi)^3 h}{2(\xi + 1 - \eta)^3} (uu_\xi - vf_\xi) \\
 \phi_\eta &= \frac{(1 + \xi)hw}{\xi + 1 - \eta} \\
 w_\eta &= \frac{w}{\xi + 1 - \eta} - \frac{3P_r(1 - \eta)(1 + \xi)^3 hfw}{2(\xi + 1 - \eta)^4} \\
 &+ \frac{3P_r\xi(1 + \xi)^3 h}{2(\xi + 1 - \eta)^3} (u\phi_\xi - wf_\xi)
 \end{aligned} \tag{27}$$

subject to

$$\begin{aligned}
 f &= 0, \quad u = 0, \quad \phi = 0 \quad \text{on } \eta = 0, \quad \xi \geq 0 \\
 f &= \frac{1}{2}, \quad v = 0, \quad w = 0 \quad \text{on } \eta = 1, \quad \xi \geq 0 \\
 h &= \frac{1}{2}, \quad f = f_0(\eta), \quad \phi = \phi_0(\eta) \quad \text{on } \xi = 0, \quad 0 < \eta \leq 1
 \end{aligned} \tag{28}$$

where the initial profiles $f_0(\eta)$ and $\phi_0(\eta)$ are found by putting $\xi = 0$ and $h = \frac{1}{2}$ into (27) and solving, subject to conditions $f = u = \phi = 0$ at $\eta = 0$ and $u = 1, \phi = 1$ at $\eta = 1$.

The parabolic system of equations and boundary conditions (27)-(28) has been solved by marching in the ξ -direction using a modification of the Keller box method. A non-uniform grid is placed on the domain $\xi \geq 0, 0 \leq \eta \leq 1$ and the resulting difference equations are solved by Newton iteration. Solutions are obtained on different sized grids and Richardson's extrapolation used to produce results of high accuracy. A full account of the numerical method and the details of implementation have fully been discussed [3].

4 RESULTS

A typical run has a coarse grid of dimension 60×48 in the (ξ, η) domain with each cell being divided into 1, 2, 3 and 4 sub-cells respectively. Because of the coordinate singularity at $\xi = 0, \eta = 1$, a non-uniform grid is employed and given by $\xi = \frac{1}{3} \sinh[\bar{\xi}^{1.5} (1 + \bar{\xi}^{1.5})]$, $\eta = 1 - (1 - \bar{\eta})^{1.5}$ where $\bar{\xi}$ and $\bar{\eta}$ are uniform. When $\Delta \bar{\xi} \equiv 0.044618955$ and $\Delta \bar{\eta} \equiv \frac{1}{47}$, this gives $\Delta \xi \sim 0.004$ and $\Delta \eta \sim 0.003$ near the singularity, which is sufficiently small to give good accuracy, and this enabled us to integrate as far as $\xi \sim 10^9$, which is necessary for the profile at infinity to be determined with sufficient accuracy. From the convergence of the extrapolation process the absolute error is 9×10^{-7} . A typical set of numerical data is presented in Table 1.

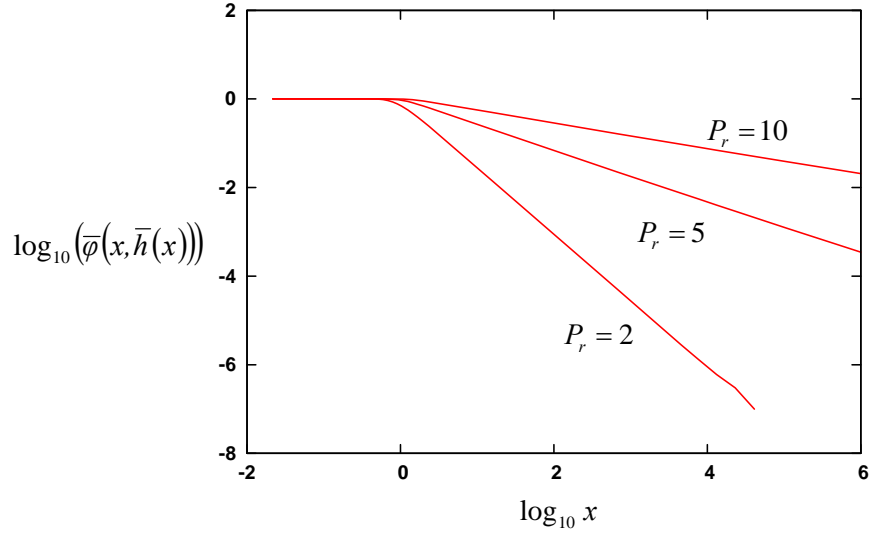
Table 1: Film thickness, free surface velocity and temperature for the axisymmetric flat plate with $P_r = 2$

x	film thickness $\bar{h}(x)$	free surface velocity $\bar{u}(x, \bar{h}(x))$	free surface temperature $\bar{\phi}(x, \bar{h}(x))$
0.000	0.500	1.000	1.000
0.115	0.539	1.000	1.000
0.197	0.587	1.000	1.000
0.294	0.659	1.000	1.000
0.416	0.767	0.981	0.999
0.520	0.875	0.911	0.989
0.733	1.191	0.682	0.891
1.072	2.206	0.368	0.660
1.669	6.338	0.128	0.389
1.968	9.930	8.188×10^{-2}	0.310
2.817	27.742	2.931×10^{-2}	0.185
5.228	1.735×10^2	4.685×10^{-3}	7.372×10^{-2}
10.791	1.520×10^3	5.348×10^{-4}	2.484×10^{-2}
25.010	1.892×10^4	4.297×10^{-5}	7.031×10^{-3}
46.931	1.250×10^5	6.504×10^{-6}	2.734×10^{-3}
1.347×10^2	2.957×10^6	2.749×10^{-7}	5.620×10^{-4}

1.073×10^3	1.495×10^9	5.438×10^{-10}	2.500×10^{-5}
1.321×10^4	2.784×10^{12}	2.920×10^{-13}	6.00×10^{-7}
1.385×10^5	3.212×10^{15}	2.531×10^{-16}	0.000
1.000×10^6	1.209×10^{18}	6.723×10^{-19}	0.000

Figure 2 shows free surface temperature for various Prandtl numbers. As P_r increases, the temperature decrease becomes more gradual.

Figure 2: Free surface temperature for various Prandtl numbers



5 CONCLUDING REMARKS

Numerical solutions of high accuracy for the flow of a cold axisymmetric vertical jet against a horizontal, flat plate have been obtained for large Reynolds numbers using the modified Keller box method. Here it is to demonstrate the successful, robust Keller-box algorithm, which provides a satisfactory methodology for the assessment of practical configurations, sufficient for the purposes of engineering practice.

REFERENCES

- [1] E.J. Watson, The radial spread of a liquid jet over a horizontal plane. *Journal of Fluid Mechanics* **20**(3), pp. 481-499 (1964)
- [2] Z.H. Chaudhury, Heat transfer in a radial liquid jet. *Journal of Fluid Mechanics* **20**(3), pp. 501-511 (1964)
- [3] J.-J. Shu and G. Wilks, Heat transfer in the flow of a cold, two-dimensional vertical liquid jet against a hot, horizontal plate. *International Journal of Heat and Mass Transfer* **39**(16), pp. 3367-3379 (1996)
- [4] Y.H. Zhao, T. Masuoka, T. Tsuruta and C.F. Ma, Conjugated heat transfer on a horizontal surface impinged by circular free-surface liquid jet. *JSME International*

Journal Series B-Fluids and Thermal Engineering **45**(2), pp. 307-314 (2002)

[5] D.R.S. Guerra, J. Su and A.P.S. Freire, The near wall behavior of an impinging jet. *International Journal of Heat And Mass Transfer* **48**(14), pp. 2829-2840 (2005)

[6] J. Rice, A. Faghri and B. Cetegen, Analysis of a free surface film from a controlled liquid impinging jet over a rotating disk including conjugate effects, with and without evaporation. *International Journal of Heat and Mass Transfer* **48**(25-26), pp. 5192-5204 (2005)